Estimating the Capacity Value of Concentrating Solar Power Plants with Thermal Energy Storage: A Case Study of the Southwestern United States

Seyed Hossein Madaeni, *Student Member, IEEE* Ramteen Sioshansi, *Member, IEEE,* and Paul Denholm, *Senior Member, IEEE*

***Abstract*—We estimate the capacity value of concentrating solar power (CSP) plants with thermal energy storage (TES) in the southwestern U.S. Our results show that incorporating TES in CSP plants significantly increases their capacity value. While CSP plants without TES have capacity values ranging between 60% and 86% of maximum capacity, plants with TES can have capacity values between 79% and 92%. We demonstrate the effect of location and configuration on the operation and capacity value of CSP plants. We also show that using a capacity payment mechanism can increase the capacity value of CSP, since the capacity value of CSP is highly sensitive to operational decisions and energy prices are not a perfect indicator of scarcity of supply.**

***Index Terms*—Capacity value, equivalent conventional power, concentrating solar power**

I. Nomenclature

A. Optimization Model Sets and Parameters

- T index set for time
- T' index set for shortage event hours
- τ^- minimum operating level of powerblock when it is online
- τ^+ maximum operating level of powerblock when it is online
- $\bar{u}$ minimum up-time of powerblock when it is started up
- $\bar{s}$ maximum amount of energy that can be charged into thermal energy storage (TES) during one hour
- $\bar{d}$ maximum amount of energy that can be discharged from TES during one hour
- η hours of storage in TES system
- e^{SU} thermal energy required to startup powerblock
- $f(\tau)$ powerblock heat rate function
- $P_h(d)$ heat transfer fluid pump parasitic load function
- ρ amount of thermal energy retained by the TES system from one hour to the next
- ϕ roundtrip efficiency of TES system
- $P_b(\tau)$ powerblock parasitic load function
- e_t^{SF} thermal energy collected by the solar field of the concentrating solar power (CSP) plant at hour t
- c variable generation cost of CSP plant
- M_t^e energy price at hour t
- M^K capacity price
- K^p capacity shortfall penalty factor

B. Optimization Model Variables

- τ_t thermal energy delivered to powerblock at hour t
- e_t net electric output of CSP plant at hour t
- l_t amount of energy in TES system at end of hour t
- s_t amount of thermal energy charged into TES in hour t
- d_t amount of thermal energy discharged from TES in hour t
- r_t binary variable that equals 1 if powerblock is started up in hour t, equals 0 otherwise
- u_t binary variable that equals 1 if powerblock is online in hour t, equals 0 otherwise
- τ_t^μ maximum thermal energy that can be delivered to the powerblock in hour t
- e_t^μ maximum potential electric output of CSP plant in hour t
- d_t^μ maximum thermal energy that can discharged from TES in hour t
- K^l capacity sold by the CSP plant in the capacity market
- K_t^r capacity shortfall during hour t

C. Capacity Value Estimation Variables and Parameters

- $\tilde{T}$ highest-load or -LOLP hours used for capacity value estimation
- p_t loss of load probability (LOLP) in hour t
- G_t conventional generating capacity available in hour t
- B_t output of benchmark plant in hour t
- L_t hour-t load
- E^C loss of load expectation (LOLE) when CSP plant is added to the system
- E^B LOLE when benchmark plant is added to the system
- $\bar{C}$ nameplate capacity of CSP plant
- w_t LOLP-based weight used in hour t
- S set of solar multiples examined
- Ψ set of hours of TES examined
- Λ set of locations examined
- $v_{s,\psi,\lambda}^E$ equivalent conventional power of a CSP plant at location λ with a solar multiple of s and ψ hours of TES
- $v_{s,\psi,\lambda}^C$ capacity factor-based approximation of a CSP plant at location λ with a solar multiple of s and ψ hours of TES

This work was supported by the U.S. Department of Energy through prime contract DE-AC36-08GO28308 and by the Alliance for Sustainable Energy, LLC through subcontract AGJ-0-40267-01.

S. Madaeni and R. Sioshansi are with the Integrated Systems Engineering Department, The Ohio State University, Columbus, OH 43210, USA (e-mail: madaeni.1@osu.edu and sioshansi.1@osu.edu).

P. Denholm is with the Strategic Energy Analysis Center, National Renewable Energy Laboratory, Golden, CO 80401, USA (e-mail: paul.denholm@nrel.gov).

II. Introduction

RESOURCE adequacy is an important issue with which power system planners contend [1]. Renewables provide an alternative to traditional sources of capacity and energy. Some renewables pose capacity planning challenges, however, due to variable and uncertain real-time output [2]–[6]. Thus accurate capacity value estimates of such resources are vital for long-term planning purposes.

Due to excellent solar resource availability, the southwestern U.S. has great potential for concentrating solar power (CSP) development, with a number of plants currently operational and others in development. Although the capacity value of CSP plants without thermal energy storage (TES) has been analyzed [7], TES is a promising technology that can increase the capacity value of CSP. This paper uses a model to optimize the operation of a CSP plant with TES and applies reliability-based and approximation techniques to estimate the capacity value of CSP plants at a number of locations in the southwestern U.S. We show that TES can significantly increase a plant's capacity value—plants without TES have capacity values between 60% and 86% of maximum capacity, whereas adding one hour of TES can increase the capacity value to between 79% and 90%. We also examine the effect of capacity payments, demonstrating that they can increase the capacity value of CSP. This is because the capacity value of CSP with TES is highly sensitive to operational decisions and energy prices are not a perfect signal of system capacity scarcity. The remainder of this paper is organized as follows: section III describes CSP technology and the model used to optimize the operation of the CSP plants, section IV discusses the capacity value estimation methods used in our analysis, section V provides details of our case study, section VI summarizes our results, section VII examines the effect of some of our assumptions, and section VIII concludes.

III. CSP Model

CSP plants consist of three separate but interrelated parts: a solar field, which collects solar thermal energy; a powerblock, which uses a heat engine to convert the thermal energy into electricity; and a TES system, which can store thermal energy collected by the solar field for later use. There are also hybridized CSP plants that include a fossil-fueled backup system. Since our analysis only considers pure CSP plants, we exclude such systems from this discussion.

One common CSP plant design is a parabolic trough system [8]–[10]. The solar field of such a plant consists of trough-shaped mirrors, which concentrate the thermal energy of sunlight onto a heat-transfer fluid (HTF). The HTF is circulated through the field and is used to drive the powerblock. Another design is a power tower, which consists of a field of mirrors, called heliostats, that concentrate sunlight on an HTF at the top of a tower in the center of the field. Although our analysis assumes parabolic trough technology, our approach is sufficiently general that it can be applied to trough designs.

TES has several advantages compared to mechanical or chemical storage technologies. TES typically has very low capital costs, with recent estimates between $72 and $240 per kWh [11]. Moreover, demonstration CSP plants with large TES systems, that can be charged and discharged for many hours, have shown high roundtrip efficiencies, often in excess of 98% [12], [13]. This can be compared to electrochemical battery storage, which can cost upwards of $300 per kWh (excluding high-cost power conversion equipment) and tend to have lower efficiencies [14]. TES is significantly more efficient because the thermal energy does not have to go through a conversion process to be stored or discharged. Rather, heat exchangers transfer the thermal energy between the HTF in the plant and a storage medium, which is typically a molten salt. One standard TES design, which our analysis considers, is a two-tank indirect system, which consists of two storage tanks (one hot, the other cold) [13], [15], [16]. When energy is stored, the HTF flows through heat exchangers and the salt flows from the cold to hot tank while being heated by the HTF. Energy is discharged by operating the system in reverse and the salt is used to heat the HTF. Other TES technologies are under development and could further reduce costs [16]–[19].

The three components of the CSP plant can be sized differently, affecting the operation and capacity value of the plant. The size of the powerblock is typically measured based on its rated output, measured in MW of electricity (MW-e). The size of the solar field can be measured by its solar multiple (SM) [20]. A solar field with an SM of 1.0 is sized to provide sufficient thermal energy to operate the powerblock at its rated capacity with direct normal irradiance (DNI) of 950 W/m^2, a wind speed of 5 m/s, and an ambient temperature of 25° C. TES has both a power and an energy capacity. The power capacity of TES is typically set to allow the powerblock to operate at maximum capacity using energy discharged from TES only, and we make this assumption. The energy capacity can be measured in terms of the number of consecutive hours that the TES system can be charged at its power capacity before filling the system, which is the convention we use. Hours of storage is occasionally defined as the number of consecutive hours that a fully-charged TES system can be discharged. Due to the high roundtrip efficiency of TES, these two definitions are similar. Because the solar field and TES system are sized in relation to the powerblock, we hold the powerblock size fixed in our analysis and consider plants with different SMs and hours of storage.

We optimize the operation of the CSP plants using the model that Sioshansi and Denholm [21] develop. This model is composed of two parts. We first use the Solar Advisor Model (SAM) [20], which is a dynamic model that uses weather data to determine the amount of thermal energy collected by the solar field in each hour. SAM assumes that the parabolic troughs in the solar field have a single-axis tracking system to follow the sun. It further accounts for the affect of ambient temperature, relative humidity, and other weather parameters on the efficiency of the solar field in collecting thermal energy. SAM has been validated against empirical data from the Solar Electric Generating Stations [22]. In the second part of the model the thermal energy collected by the solar field, as modeled by SAM, is input to a mixed-integer program (MIP) that optimizes the operation of the CSP plants by determining how the powerblock and TES should be operated, subject to

thermal energy availability and plant-operating constraints.

We model the CSP plants under two different market structures, which affect their operations. The first assumes an energy-only market, in which the CSP plants receive payments for only energy supplied. The second assumes that the CSP plants receive energy payments as well as supplemental payments for providing firm capacity. The formulation of the energy-only model is given by:

$$\max_{\substack{e,l,s,d,\\ \tau,r,u}} \sum_{t\in T}(M_t^e - c)\cdot e_t; \tag{1}$$

$$\text{s.t.}\quad l_t = \rho\cdot l_{t-1} + s_t - d_t, \qquad \forall\ t\in T; \tag{2}$$

$$0 \le l_t \le \eta\cdot \bar{s}, \qquad \forall\ t\in T; \tag{3}$$

$$0 \le s_t \le \bar{s}, \qquad \forall\ t\in T; \tag{4}$$

$$0 \le d_t \le \bar{d}, \qquad \forall\ t\in T; \tag{5}$$

$$s_t - \phi\cdot d_t + \tau_t + e^{SU}\cdot r_t \le e_t^{SF}, \qquad \forall\ t\in T; \tag{6}$$

$$e_t = f(\tau_t) - P_h(d_t) - P_b(\tau_t), \qquad \forall\ t\in T; \tag{7}$$

$$\tau^-\cdot u_t \le \tau_t \le \tau^+\cdot u_t, \qquad \forall\ t\in T; \tag{8}$$

$$r_t \ge u_t - u_{t-1}, \qquad \forall\ t\in T; \tag{9}$$

$$u_t \ge \sum_{\xi=t-\bar{u}}^{t} r_\xi, \qquad \forall\ t\in T; \tag{10}$$

$$u_t, r_t \in \{0,1\}; \qquad \forall\ t\in T. \tag{11}$$

Objective function (1) maximizes revenues from energy sales less variable generation costs. Constraints (2) through (5) impose restrictions on the TES system. Constraints (2) define the storage level in each hour in terms of the previous storage level, less thermal energy losses, and current-hour storage and discharge decisions. Constraints (3) impose the energy restrictions, and constraints (4) and (5) impose power restrictions. Constraints (6) restrict the amount of thermal energy used in net in each hour to be less than the amount collected by the solar field. Constraints (7) define net generation at each hour to equal gross powerblock output less parasitic loads. The heat rate and parasitic load functions in constraints (7) account for the effects of weather on powerblock efficiency. Constraints (8) impose the minimum and maximum output restrictions when the powerblock is online, fixing powerblock output to zero otherwise. Constraints (9) define the powerblock startup state variables in terms of changes in online state variables, while constraints (10) enforce the minimum up-time restriction when the powerblock is started up. Constraints (11) impose the integrality restriction on the state variables.

While scarcity pricing in an energy-only spot market theoretically signals the need for additional capacity, such signals are not perfect in practice. Some markets employ capacity (in addition to energy) payments to induce generation to enter the market and provide capacity when it is needed in real-time. Since such payments are subject to performance requirements, they could provide stronger incentives for a CSP plant to have energy available when it is most needed—thereby improving the plant's capacity value—which we explore in section VII.

Although the details of capacity payment mechanisms differ between markets, they all have some common elements. Generally, generators contract with the system operator (SO) to provide capacity over some fixed time period for a payment per MW of capacity provided. The generator must have the contracted capacity available during SO-designated shortage events, otherwise it is subject to financial penalties. Most markets set the capacity payment price and non-performance penalties using a combination of a capacity auction and administrative rules. Following the design of ISO New England's Forward Capacity Market we assume that if the CSP plant contracts to provide capacity that cannot be delivered during a shortage event, a penalty based on the percentage of the contracted capacity not provided is levied.

When the capacity payments and penalties are included, the CSP optimization model becomes:

$$\max_{\substack{e,l,s,d,\tau,r,\\ u,K^l,K_t^r}} \sum_{t\in T}(M_t^e - c)\cdot e_t + M^K K^l - M^K K^p \sum_{t\in T'}\frac{K_t^r}{K^l} \tag{12}$$

$$\text{s.t.}\quad \text{constraints (2) through (11);} \tag{13}$$

$$K_t^r \ge K^l - e_t^\mu, \qquad \forall\ t\in T; \tag{14}$$

$$d_t^\mu \le \min\left\{\rho\cdot l_{t-1}, \bar{d}\right\}, \qquad \forall\ t\in T; \tag{15}$$

$$-\phi\cdot d_t^\mu + \tau_t^\mu + e^{SU}\cdot r_t \le e_t^{SF}, \qquad \forall\ t\in T; \tag{16}$$

$$e_t^\mu = f(\tau_t^\mu) - P_h(d_t^\mu) - P_b(\tau_t^\mu), \qquad \forall\ t\in T; \tag{17}$$

$$\tau^-\cdot u_t \le \tau_t^\mu \le \tau^+\cdot u_t, \qquad \forall\ t\in T; \tag{18}$$

$$K_t^r, d_t^\mu, K^l \ge 0, \qquad \forall\ t\in T. \tag{19}$$

Objective function (12) maximizes the sum of energy and capacity payments, less penalties for non-performance in the capacity market. Constraints (2) through (11) are included since the underlying operating capabilities of the plant are unchanged when capacity payments are included. Constraints (14) through (19) define the maximum amount of energy that the CSP plant can generate in each hour and the resulting capacity shortfall. Constraints (14) define the hour-t capacity shortfall to at least equal the difference between the contracted quantity and the maximum amount of energy that the plant can feasibly produce in hour t. Constraints (15) define the maximum amount of energy that can be discharged from TES in each hour to be the minimum of the discharge capacity and the energy in TES carried over from the previous hour. Constraints (16) define the maximum amount of thermal energy that can be delivered to the powerblock in each hour based on the solar field energy and energy in TES. Constraints (17) define the maximum amount of electricity that can be generated in each hour based on the amount of thermal energy that can be feasibly delivered to the powerblock. Constraints (18) and (19) impose minimum and maximum powerblock loading and non-negativity restrictions. Constraints (18) further require the powerblock to be online to provide capacity to the system in a given hour.

These types of 'price-taking' models yield dispatch pattern that are generally similar to demand patterns. In summer months output tends to peak in the late afternoon, whereas in the winter a morning and evening peak is often observed due to demand peaks driven by lighting and heating loads. Sioshansi and Denholm [21], [23] and Madaeni *et al.* [7] provide examples of CSP dispatch patterns during different

periods of the year.

IV. Capacity Value Estimation Methods

A. Reliability-Based Method

Numerous techniques have been used to approximate the capacity value of conventional and renewable generators. Reliability-based methods are among the most robust and widely accepted of these [6], [7], [24]–[30]. These techniques use a standard power system reliability index, loss of load probability (LOLP), to determine how a generator affects the reliability of the system. LOLP is defined as the probability that generator or transmission outages leave the system with insufficient capacity to serve the load in a given hour. A related reliability index, loss of load expectation (LOLE), is defined as the sum of LOLPs over some planning horizon, and gives the expected number of outage hours within that horizon. Conventional generator and transmission outages are typically modeled using an equivalent forced outage rate (EFOR), which captures the probability of a failure at any given time. With variable renewables, one must model mechanical failures using an EFOR and capture resource variability. The latter is typically done using historical resource data or by simulating such data from underlying probability distributions. Reliability-based methods determine the capacity value of a generator by how it affects the system's LOLPs and LOLE.

Standard reliability-based methods include the effective load-carrying capability (ELCC), equivalent firm power (EFP), and equivalent conventional power (ECP), which is the reliability-based metric that we focus on. The ELCC of a generator is defined as the amount by which system loads can increase when the generator is added while maintaining the same LOLE [31]. The EFC of a generator, g, is defined to be the capacity of a fully reliable generator (*i.e.* with a 0% EFOR) that can replace g while maintaining the same LOLE [32], [33]. A generator will generally have a different ELCC and EFC since changing the generation mix of a system will change the probability distribution of available generating capacity in an hour, whereas changing loads will not [30]. ECP is similar to EFC, except that the generator against which g is benchmarked is not fully reliable and instead assumed to have a positive EFOR. This metric is particularly attractive for renewable generators, since it allows the capacity value to be compared to a conventional dispatchable resource. For instance, one may find that a 100 MW wind plant has a capacity value that is equivalent to a 30 MW natural gas-fired combustion turbine, which corresponds to a 30% ECP.

Estimating the capacity value of a CSP plant with TES is complicated by the fact that one must account for both the energy that the plant actually plans to generate, as well as stored energy. This is because if a system shortage event is to occur, stored energy could be used to increase the output of the CSP plant and help mitigate the capacity shortfall. Tuohy and O'Malley [34] propose a capacity value approximation technique for pumped hydroelectric storage (PHS) that we apply to a CSP plant with TES. Their method determines an optimal (*e.g.* revenue-maximizing) dispatch of the PHS plant subject to technical constraints. They then determine, based on this dispatch and the amount of energy in storage in each hour, the maximum amount of energy that the PHS could feasibly generate in a subset of hours during which the system has a high likelihood of experiencing an outage. This maximum potential generation is used to estimate the capacity value of the plant. In our analysis, we focus on the 10 hours of each year with the highest LOLPs, since the capacity value of CSP without TES is most sensitive to its operation during these most critical hours [7]. This can be contrasted with wind, which can require up to the top 900 hours of the year to be considered to accurately estimate its capacity value [3].

To apply this method to CSP, we first define the maximum amount of energy that can be generated by the CSP plant in each hour, based on the optimized operation of the plant. In the case with capacity payments, this quantity is defined endogenously by the optimized values of the e_t^μ variables. In the case with only energy payments, we compute this by first defining the maximum amount of thermal energy that could be delivered to the powerblock in each hour as:

$$\begin{aligned}\tau_t^\mu \quad = \quad & u_t \cdot \max\left\{0, \min\left\{\tau^+, e_t^{SF} - e^{SU} \cdot r_t \right.\right. \\ & \left.\left. +\phi \cdot \min\left\{\bar{d}, \rho \cdot l_{t-1}\right\}\right\}\right\}. \end{aligned} \tag{20}$$

Equation (20) defines τ_t^μ as the minimum of the powerblock's rated capacity and the sum of the thermal energy collected by the solar field and energy available in TES. Equation (20) further assumes that the powerblock must be online in order to generate energy, precluding the possibility of an immediate emergency startup during a contingency event. We explore the effects of relaxing this assumption in section VI.

We next determine the amount of τ_t^μ that is taken out of TES as:

$$d_t^\mu = \max\left\{0, \tau_t^\mu - e_t^{SF}\right\}. \tag{21}$$

We finally define the maximum potential generation of the CSP plant in each hour as:

$$e_t^\mu = f(\tau_t^\mu) - P_h(d_t^\mu) - P_b(\tau_t^\mu). \tag{22}$$

To estimate the CSP plant's ECP, we first compute the LOLPs of the base system without the CSP plant as the probability that the load cannot be met by the existing generators:

$$p_t = \text{Prob}\left\{G_t < L_t\right\}, \tag{23}$$

where the probability function accounts for the likelihood of outages. We let $\tilde{T}$ denote the subset of hours with the highest LOLPs, which are considered for the capacity value estimation. We then compute the LOLE when the CSP plant is added to the system as:

$$E^C = \sum_{t \in \tilde{T}} \text{Prob}\left\{G_t + e_t^\mu < L_t\right\}. \tag{24}$$

We also compute the LOLE when a benchmark unit only (*i.e.* without the CSP plant) is added to the system as:

$$E^B = \sum_{t \in \tilde{T}} \text{Prob}\left\{G_t + B_t < L_t\right\}. \tag{25}$$

The ECP of the system is found by adjusting the nameplate capacity of the benchmark unit until:

$$E^C = E^B. \tag{26}$$

B. Capacity Factor-Based Approximation Method

Although reliability-based methods, such as ECP, provide robust capacity value estimates, they require detailed system data. They can also be computationally expensive, since LOLPs must be iteratively recalculated until achieving condition (26). This is less of an issue today, however, with computational resources currently available [35]. As such, approximation techniques have been developed. One such class of techniques, which we call capacity factor-based approximations, consider the capacity factor of a generator over a subset of hours during which the system faces a high risk of a shortage—for instance hours with high loads or LOLPs.[1] A generator's capacity factor is defined as its average output during a set of hours divided by its maximum capacity. A number of studies apply capacity factor-based approximations to wind [3], [36], [37] and photovoltaic solar [38], comparing them with reliability-based methods to assess their accuracy. Madaeni *et al*. [7] compare the accuracy of applying different capacity factor-based approximations as opposed to reliability-based methods to CSP plants without TES. They approximate the capacity value of CSP as the average capacity factor during the 10 and 100 hours of each year with the highest loads and LOLPs, where the LOLPs of the base system without the CSP plant added are used. We refer to these as the top-load and -LOLP methods. They also examine a method, which we refer to as the LOLP-weighted method, which uses a weighted average capacity factor during the highest-load hours, with the LOLPs used as weights. They show that the LOLP-weighted method provides the closest approximation of the reliability-based methods, and that using the 10 highest-load hours of the year provides the best approximation.

We compare ECP and capacity factor-based approximations using the 10 hours of each year with the highest loads and LOLPs, as well as the LOLP-weighted method. The top-load and -LOLP methods approximate a plant's capacity value as:

$$\frac{\sum_{t \in \tilde{T}} e_t^{\mu}}{|\tilde{T}| \cdot \bar{C}}, \tag{27}$$

where $\tilde{T}$ is the set of hours with the highest system loads or LOLPs and $|\tilde{T}|$ is the cardinality of $\tilde{T}$. The weights used in the LOLP-weighted approximation are:

$$w_t = \frac{p_t}{\sum_{\xi \in \tilde{T}} p_\xi}. \tag{28}$$

The LOLP-weighted approximation of the capacity value is then given by:

$$\frac{\sum_{t \in \tilde{T}} w_t \cdot e_t^{\mu}}{\bar{C}}. \tag{29}$$

V. Case Study

We estimate the capacity values of CSP plants at three sites in the southwestern U.S., which are listed in Table I, using historical conventional generator, load, and weather data from 1998 to 2005. The capacity values of CSP plants without TES have significant interannual variability [7], and studying eight years provides a more robust long-term estimate. We study these locations in isolation, considering a CSP plant added to each site individually. Thus our capacity value estimates are not additive, since they do not account for correlation in weather conditions between the locations. Moreover, our capacity values are calculated by assuming a single CSP plant is added and do not account for the fact that the marginal capacity value of CSP decreases as more CSP capacity is added to the system. Our estimates also neglect transmission constraints, which can reduce the capacity value of CSP if there is insufficient capacity to deliver power to loads. Our estimates use hourly data as the capacity value of CSP plants without TES is relatively insensitive to subhourly resource variability, and we expect this to be true of plants with TES [7].

TABLE I
Location of CSP Plants Studied

CSP Site	Coordinates
Thermal, California	33.65° N, 116.05° W
Amargosa Valley, Nevada	36.55° N, 116.45° W
Magdalena, New Mexico	34.35° N, 107.35° W

A. CSP Plants and Operation

Our analysis assumes that the components and performance of the CSP plants correspond to the default trough system modeled in version 2.0 of SAM [20]. This plant has a 110 MW-e wet-cooled powerblock, which can be operated at up to 115%, a two-hour powerblock minimum up-time, non-linear parasitic loads, and no auxiliary fossil-fueled heat source. When the parasitic component loads are taken into account, the maximum net electric output of the CSP plant is about 120 MW-e. We use this 120 MW-e maximum net output to normalize the capacity values of the plants. The default CSP plant in SAM has a 6% EFOR, which we assume.

In order to make our model computationally tractable, we optimize the operation of the CSP plants one day at a time using a rolling 48-hour optimization horizon. Inclusion of hours 25 through 48 in the model ensures that thermal energy that would be valuable on the subsequent day is kept in TES at the end of hour 24 [39]. We further assume that price and weather data are perfectly known to the plant operator *a priori*. Sioshansi and Denholm [21] use a 'backcasting' heuristic to demonstrate that the operation and profitability of CSP are relatively insensitive to these assumptions. This heuristic determines the operation of a plant on each day by assuming that prices and solar availability from the previous day will repeat themselves and can capture at least 87% of the profits that are possible with perfect foresight. The heuristic works well because price patterns are relatively similar from one day to the next.

B. Data Sources

Since the locations that we study are in the Western Electricity Coordinating Council (WECC) region, we model the

[1] Although loads and LOLPs are correlated, they are not perfectly coincident, since generator EFORs and capacities can vary seasonally due to factors such as planned maintenance outages and water inflows to hydroelectric plants.

entire WECC to determine LOLPs. Since we use the same underlying system in our calculations, capacity value differences between the locations are solely due to solar resource and CSP dispatch differences. System planners often use more limited regions in capacity planning, however. Because the capacity value of CSP depends on the relationship between LOLPs and generation patterns, the capacity value of a CSP plant may differ depending on whether a more limited study region is used.

WECC LOLPs are estimated by calculating the system's capacity outage table, which assumes that generator outages follow Bernoulli distributions that are serially and jointly independent [24]. Data requirements and sources used in our calculations are detailed below.

1) Conventional Generators: The rated capacities of conventional generators are obtained from Form 860 data collected by the U.S. Department of Energy's Energy Information Administration. Form 860 reports winter and summer capacities for each generator, which we use in our analysis. The WECC had between 1,016 and 1,622 generating units and 123 GW and 163 GW of generating capacity during the years that we study, reflecting load growth during this period.

We model generator outages using a simple two-state (online/offline) model. We use the North American Electric Reliability Corporation's Generating Availability Data System (GADS) to estimate generator EFORs. The GADS specifies historical annual average EFORs for generators based on generating capacity and technology, which we combine with generating technology data given in Form 860. The EFORs used range between 2% and 17% and have a capacity-weighted average of 7% for the entire WECC.

2) Load: Hourly historical load data for each year are obtained from Form 714 filings with the Federal Energy Regulatory Commission (FERC). Form 714 includes load reports for nearly all of the load-serving entities (LSEs) and utilities in the WECC, although some small municipalities and cooperatives are not included. We assume loads are fixed and deterministic based on these data, which have annual peaks ranging between 107 GW and 124 GW. Since the system loads increased over the study period and capacity expansion can lead or lag such growth, we adjust the hourly load profiles in each year individually so that the LOLPs of the base system in each year sum to 2.4. This corresponds to the standard planning target of one outage-day every 10 years [40]. This load adjustment is done by scaling all of the hourly loads by a fixed percentage, ranging between 0.1% and 5% in the different years.

3) Prices: In the energy-only market, the operations of the CSP plants is optimized to maximize energy revenues. Hourly day-ahead prices for the California ISO's SP15 zone are used to optimize the plant in California. Hourly load lambda data, obtained from FERC Form 714 filings by Nevada Power and Public Service Company of New Mexico, are used for the other locations.

The capacity market case is modeled by assuming that the plant receives a supplemental fixed payment for its contracted capacity, which carries an obligation to be able to provide energy during SO-designated shortage events. The capacity price is assumed to be set based on the capital cost of a natural gas-fired combustion turbine (NGCT), since such generators are often used for peak-capacity purposes. We assume an NGCT cost of $625/kW in 2005 dollars [41] and use a capital charge rate (CCR) to convert this total capital cost into an annualized cost [42]. Using an 11% CCR yields an annualized capacity payment of $M^K = $68.75/kW-year. Most SOs define shortage events as hours with low operating reserves, since that is when the system faces the highest probability of a system outage. We assume that the 10 hours of each year with the highest LOLPs are shortage event hours. The penalty price for not providing contracted capacity is assumed to be half of the annualized capacity cost (*i.e.* $K^p = $34.38/kW-year). All of the capacity payments and penalties are deflated to 1998 through 2005 dollars using consumer price index data reported by the U.S. Bureau of Labor Statistics. The capacity payment and penalty parameters used are based on the design of the Forward Capacity Market operated by ISO New England.

4) Weather: SAM requires detailed weather data, including DNI, dry-bulb and dew-point temperatures, relative humidity, barometric pressure, and wind speed. These data are obtained from the National Solar Radiation Data Base [43], which accounts for cloud cover and other factors in determining local weather conditions.

VI. Capacity Value Estimates

Fig. 1 shows the average (over the years 1998 to 2005) annual capacity values of a CSP plant with an SM of 1.9 at the California location in an energy-only market. ECPs and capacity factor-based approximations, which are reported as percentages of the 120 MW-e maximum net output of the plant, are given. The figure shows that TES can increase the plant's capacity value by up to 7%. It also shows that the LOLP-weighted method provides the best approximation of the ECP, with similar results for CSP plants at the other locations and with different configurations. Madaeni *et al*. [7] compare the different capacity factor-based approximations using a root mean squared error (RMSE) metric, which is defined as:

$$\sqrt{\frac{1}{|S| \cdot |\Psi| \cdot |\Lambda|} \sum_{s \in S} \sum_{\psi \in \Psi} \sum_{\lambda \in \Lambda} \left(v^E_{s,\psi,\lambda} - v^C_{s,\psi,\lambda} \right)^2}. \qquad (30)$$

The LOLP-weighted method has an RMSE of 0.71 as opposed to 2.62 and 2.61 for the top-load and -LOLP methods, respectively.

Fig. 2 through 4 show average annual LOLP-weighted approximations for CSP plants with different configurations at all three locations in an energy-only market. They show the sensitivity of the capacity value to both plant location and size, and that the values can range between 61% and 91%. A larger solar field increases total plant generation, whereas TES allows generation to be shifted to higher-priced hours. Since prices are correlated with supply scarcity, which is related to system LOLPs, this generation shifting increases capacity values. Energy prices in California provide relatively strong scarcity signals, which is theoretically true of energy spot markets [44]. Conversely, the Nevada and New Mexico

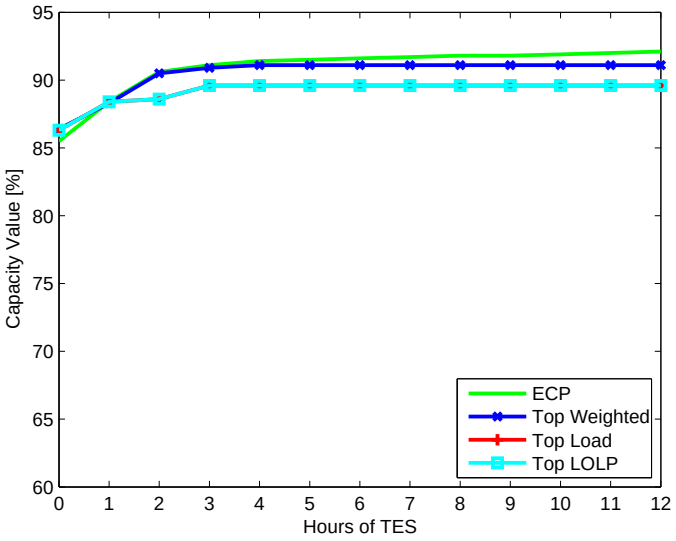

Fig. 1. Average (over the years 1998 to 2005) annual capacity value of a CSP plant with SM of 1.9 at the California location, as a percentage of 120 MW-e maximum net output of the plant. ECPs and capacity factor-based approximations are given.

plants are dispatched against load lambda data, which do not incorporate such factors. Thus these plants have weaker signals to have energy in storage and be online during high-LOLP hours. Indeed, although the New Mexico plant has lower capacity values, its energy yield is about 0.5% higher than the plant in California. The figures also show that the marginal value of TES quickly tapers off after about two to three hours of storage. This is because energy prices and LOLPs are not perfectly correlated, thus there are high-LOLP hours during which it is less profitable for CSP to generate.

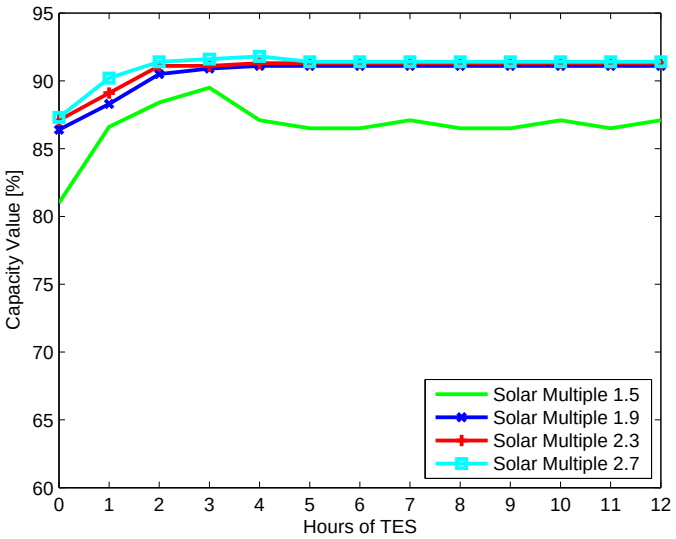

Fig. 2. Average annual LOLP-weighted approximation for a CSP plant at the California location, as a percentage of 120 MW-e maximum net output of the plant.

Fig. 1 through 4 also show that the relationship between plant size and capacity value is not perfectly monotone. This non-monotonicity is because changing the configuration of a CSP plant can affect its operation, resulting in the plant being

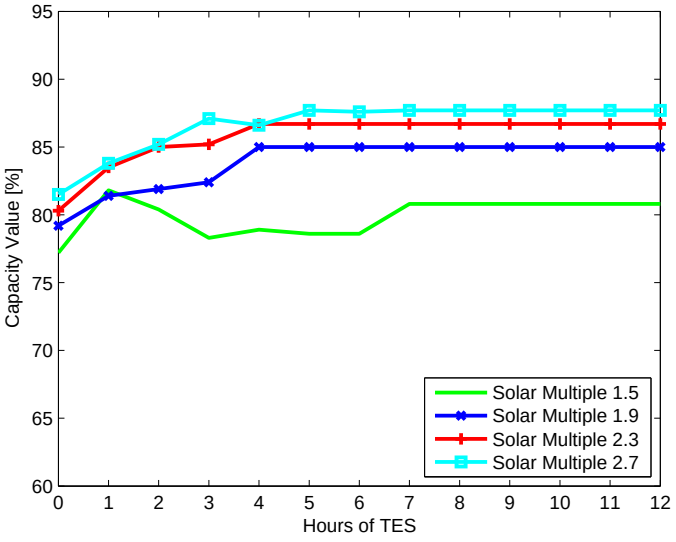

Fig. 3. Average annual LOLP-weighted approximation for a CSP plant at the Nevada location, as a percentage of 120 MW-e maximum net output of the plant.

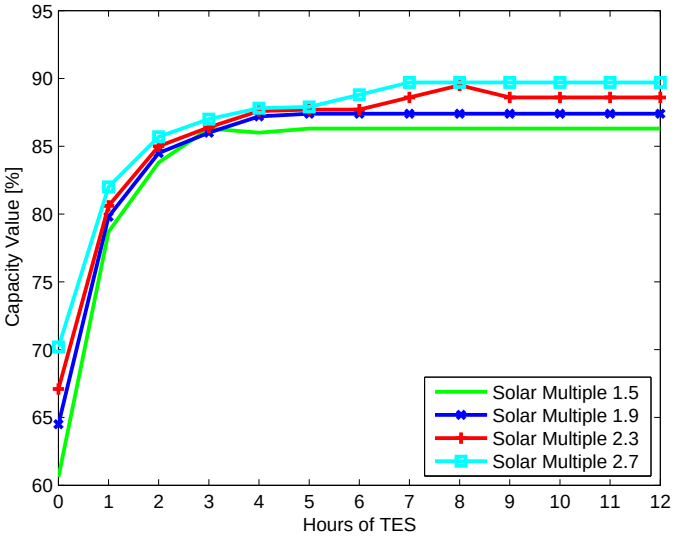

Fig. 4. Average annual LOLP-weighted approximation for a CSP plant at the New Mexico location, as a percentage of 120 MW-e maximum net output of the plant.

offline or having less energy in TES during a critical hour when the system has a high LOLP. To further illustrate these effects, Fig. 5 summarizes the operation of CSP plants with four hours of TES and SMs of 2.2 and 2.7 in Nevada on July 12, 1999—a day with relatively high LOLPs—and on the previous day. The figure shows LOLPs and the amount of thermal energy available from TES and the solar field in each hour. Contrasting the profiles of the two plants shows that the larger CSP plant with an SM of 2.7 has less stored energy available on July 12 and, importantly, during the high-LOLP hours of the afternoon. The reason for this is that this plant was able to startup and generate electricity during high-priced hours in the afternoon of the previous day. The plant with an SM of 2.2 was not able to due to the powerblock minimum-load and up-time constraints, and as such more energy is kept

in TES, yielding the higher capacity value. Similarly, a larger TES system can affect the operation of a plant, for instance allowing it to startup during a high-priced hour due to more stored energy being available. This reduces the amount of stored energy available in subsequent hours, which can reduce the plant's capacity value.

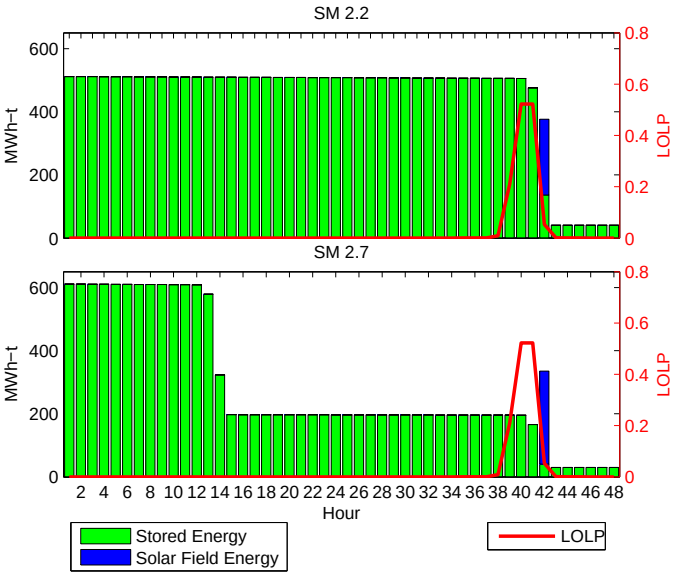

Fig. 5. Hourly LOLPs and energy in TES and collected by solar field of CSP plant with four hours of TES and different solar field sizes at the Nevada location on July 11–12, 1999.

In addition to increasing the capacity value of CSP, TES also reduces interannual capacity value variability. The capacity value of CSP plants without TES can have significant interannual variability, due to differences in resource availability [7]. A CSP plant with an SM of 1.5 and no TES can have an annual capacity value that ranges between 12% and 94%, depending on the year and location. Adding four hours of TES to such a plant increases the minimum annual capacity value to 38%. Table II provides summary statistics of the coefficient of variation, which is the ratio between the standard deviation and mean, of the annual capacity value of CSP plants with different amounts of TES. The summary statistics are given over the different locations and solar field sizes that we analyze. The table shows that TES can have a significant effect in reducing interannual capacity value variability—adding one hour of TES nearly halves the variability relative to a plant without TES. This can be attractive from a system planning perspective, since less variability implies that a CSP plant can be viewed as a more 'firm' resource for long-term capacity planning purposes.

TABLE II
SUMMARY STATISTICS OF COEFFICIENT OF VARIATION OF ANNUAL CSP CAPACITY VALUE

	Coefficient of Variation		
Hours of TES	Minimum	Maximum	Average
0	0.17	0.34	0.27
1	0.04	0.29	0.15
2	0.02	0.26	0.12
4	0.01	0.25	0.09
8	0.02	0.25	0.08
12	0.02	0.25	0.08

VII. Sensitivity of Capacity Values to Assumptions

A. Capacity Payments

Our analysis illustrates that the capacity value of CSP is very sensitive to signaling the need for capacity, since it is critically related to the dispatch of the plant and TES. Our analysis thus far shows that energy prices provide such signals to a limited extent, since energy prices and LOLPs are somewhat correlated. Energy prices do not provide perfect signals, however. For instance, plants in Nevada and New Mexico that are dispatched against load lambdas have relatively low capacity values due to a lack of strong scarcity signals. Even a plant in California does not attain the 94% theoretical maximum LOLP-weighted capacity value approximation (accounting for the 6% EFOR).

We use the model consisting of objective function (12) and constraints (13) through (19) to explore the benefits of a capacity payment mechanism in increasing the capacity value of CSP. To overcome computational issues raised by the nonlinear objective function, we solve the model using a grid-search method wherein we hold the value K^l fixed, solve the resulting linear MIP, and find a profit-maximizing choice of K^l. $K^l = 120$, which is the maximum generating capacity of the CSP plant, is profit-maximizing at all locations. The optimized values of the e_t^μ variables are used to compute LOLP-weighted estimates of the capacity values of the plants.

Fig. 6 shows the annual average capacity value estimates of CSP plants with SM of 1.5 when the capacity payment is included. Contrasting this with Fig. 1 through 4 shows that the capacity payment can significantly increase the capacity values. Nevertheless, the capacity values of the plants are not exactly 94% despite the plants selling 120 MW-e of capacity. This is because the non-performance penalty is less than the revenue that the plants earn from selling capacity. Thus there are high energy-price hours with low LOLPs during which the plants sell energy, with the energy revenues outweighing the associated capacity-related penalties in another high-LOLP hour.

B. Immediate CSP Startup

In deriving the maximum potential generation of the CSP plant using (18) or (20) we assume that for the CSP plant to be able to generate in hour t it must already be online. In practice, a CSP plant that would otherwise be offline, may technically be able to startup and generate energy in a system contingency or emergency situation. We bound the effect of relaxing the startup assumption by estimating the capacity value of a CSP plant that can startup immediately and generate electricity without any ramping constraints, so long as the necesssary startup energy is expended.

To do so we define the maximum amount of thermal energy

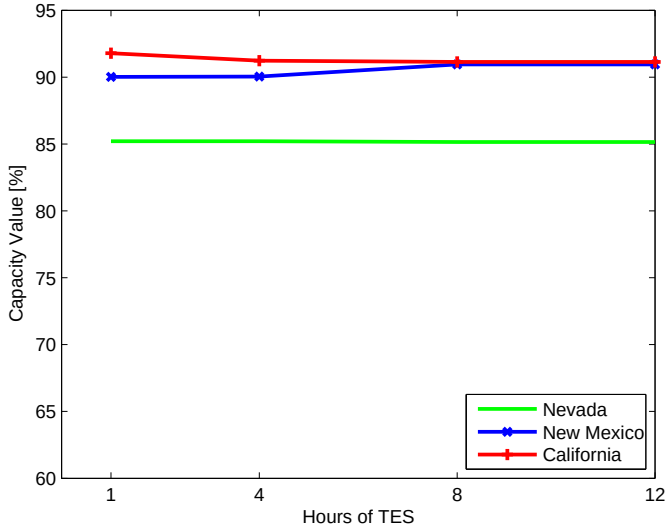

Fig. 6. Average annual LOLP-weighted approximation for CSP plants with SM of 1.5 at the three locations when a capacity payment is included, as a percentage of 120 MW-e maximum net output of the plant.

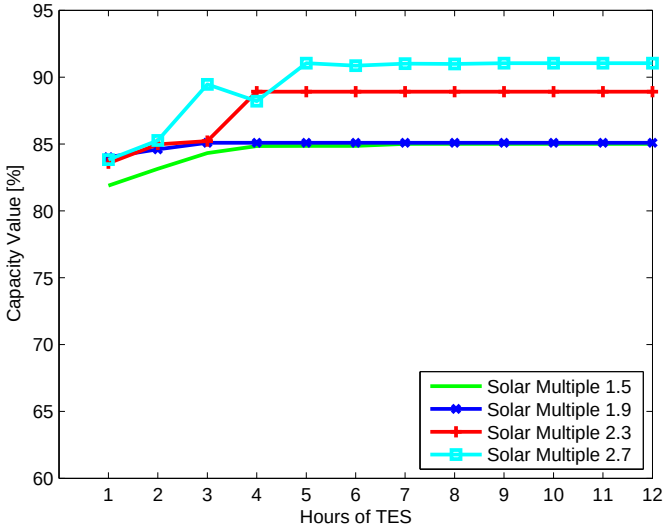

Fig. 7. Average annual LOLP-weighted approximation for a CSP plant at the Nevada location if immediate powerblock startups are allowed, as a percentage of 120 MW-e maximum net output of the plant.

that can be delivered to the powerblock in hour t as:

$$\tau_t^{\mu} = \max\left\{0, \min\left\{\tau^{+}, e_t^{SF} - e^{SU}\cdot(1+r_t-u_t) + \phi\cdot\min\left\{\bar{d}, \rho\cdot l_{t-1}\right\}\right\}\right\}. \quad (31)$$

If the powerblock is not scheduled to be online (as determined by the optimization model) in hour t, then $r_t = u_t = 0$. Thus (31) allows the powerblock to be started up and electricity to be generated, so long as e^{SU} MWh-t is used for startup energy. Otherwise, if the powerblock is already scheduled to be online, then (20) and (31) yield the same value for τ_t^{μ}. Defining τ_t^{μ} this way, the maximum potential generation of the CSP plant in each hour can be computed using (21) and (22) and an LOLP-weighted approximation can be computed as before.

Fig. 7 summarizes the capacity value of a CSP plant at the Nevada location in an energy-only market when the startup assumption is relaxed. Contrasting this with Fig. 3 shows that allowing a CSP plant to startup immediately during an system shortage event has two noticeable effects. One is that the capacity values tend to increase. The other is that the capacity values are slightly more monotone in the plant size. Both of these effects are because in some cases a CSP plant has energy in TES, but the powerblock is not online since the energy is being saved to exploit higher prices during subsequent lower-LOLP hours. If the powerblock is able to startup to provide capacity during a contingency event, this allows the energy in TES to increase the plant's capacity value. Relaxing the startup assumption has similar effects on CSP plants at the other two locations—the plants have capacity values of at least 88% and are almost completely monotone in the plant size.

VIII. Conclusions

This paper adapts an approximation method to estimate the capacity value of CSP plants with TES. We demonstrate that capacity factor-based methods can provide reasonable approximations of reliability-based methods. The LOLP-weighted method provides the best approximations, with an RMSE of 0.71. We find that only the most critical hours of each year need to be considered when estimating the capacity value of CSP. This is an important consideration, since SOs often rely on such approximation techniques to estimate the capacity value of renewables. Clearly, CSP should be treated differently than wind in such calculations. Using a case study of the southwestern U.S. we show that CSP plants with TES can have extremely high capacity values ranging between 79% and 92% of maximum capacity, as opposed to only 60% to 86% without TES. TES also reduces interannual variability in the capacity value of CSP, which can be beneficial for long-term planning. This further implies that multiple years of data may not be as crucial for estimating the capacity value of CSP with TES as it is for other renewables. Larger CSP plants tend to have higher capacity values, although this relationship is not perfectly monotone, demonstrating some of the limitations of energy prices in signaling resource scarcity. We demonstrate that including capacity payments can significantly increase capacity values, especially in the absence of organized spot markets that signal scarcity through energy prices. Similarly, designing the powerblock to be able to startup immediately during a system shortage event can significantly increase the capacity value.

Although we estimate capacity values by modeling the entire WECC system, system planners often use more limited system footprints in their analyses. This could affect the capacity value of CSP, depending on the extent to which the plant's generation is coincident with the 'local' system load. By modeling the entire WECC system we further assume that the system has sufficient transmission capacity to deliver power wherever it is needed. If binding transmission constraints prevent this, actual capacity values could be lower than our calculations suggest [45]. Further work is needed to better understand the effects of such considerations, which is an area of future research that we are pursuing.

While our analysis is limited to locations within the WECC, we expect similar capacity values, especially in plants with TES, in regions of the world with solar resources that are favorable for CSP development. Nevertheless, further research is needed to examine how CSP plants would be operated and associated capacity value implications in other systems and regions. Other areas for future research include examining the marginal capacity value of CSP as a function of penetration, and developing more detailed models of tower, linear Fresnel reflector, and dry-cooled CSP plants. These are increasingly important issues, as a number of tower plants under construction in the U.S. and internationally.

ACKNOWLEDGMENT

The authors would like to thank M. Mehos, C. Turchi, M. Milligan, A. Green, W. Short, R. Newmark, and A. Sorooshian, the editor, and five anonymous reviewers for helpful discussions and suggestions.

REFERENCES

[1] A. Keane, M. R. Milligan, C. J. Dent, B. Hasche, C. D'Annunzio, K. Dragoon, H. Holttinen, N. Samaan, L. Söder, and M. O'Malley, "Capacity value of wind power," *IEEE Transactions on Power Systems*, vol. 26, pp. 564–572, May 2011.

[2] M. R. Milligan, "Measuring wind plant capacity value," National Renewable Energy Laboratory, Tech. Rep. NREL/TP-441-20493, 1996.

[3] M. R. Milligan and B. Parsons, "Comparison and case study of capacity credit algorithms for wind power plants," *Wind Engineering*, vol. 23, pp. 159–166, May 1999.

[4] M. R. Milligan and T. Factor, "Optimizing the geographic distribution of wind plants in iowa for maximum economic benefit and reliability," *Wind Engineering*, vol. 24, pp. 271–290, July 2000.

[5] M. R. Milligan and K. Porter, "The capacity value of wind in the united states: Methods and implementation," *The Electricity Journal*, vol. 19, pp. 91–99, March 2006.

[6] G. R. Pudaruth and F. Li, "Capacity credit evaluation: A literature review," in *Third International Conference on Electric Utility Deregulation and Restructuring and Power Technologies*. Nanjing, China: Institute of Electrical and Electronics Engineers, 6-9 April 2008, pp. 2719–2724.

[7] S. H. Madaeni, R. Sioshansi, and P. Denholm, "Estimating the capacity value of concentrating solar power plants: A case study of the southwestern United States," *IEEE Transactions on Power Systems*, vol. 27, pp. 1116–1124, May 2012.

[8] H. Price, E. Lüpfert, D. Kearney, E. Zarza, G. Cohen, R. Gee, and R. Mahoney, "Advances in parabolic trough solar power technology," *Journal of Solar Energy Engineering*, vol. 124, pp. 109–125, May 2002.

[9] "Assessment of parabolic trough and power tower solar technology cost and performance forecasts," National Renewable Energy Laboratory, Tech. Rep. NREL/SR-550-34440, October 2003.

[10] M. Selig and M. Mertins, "From saturated to superheated direct solar steam generation—technical challenges and economical benefits," in *SolarPACES 2010 Conference*, Perpignan, France, 21-24 September 2010.

[11] C. Turchi, M. Mehos, C. K. Ho, and G. J. Kolb, "Current and future costs for parabolic trough and power tower systems in the us market," National Renewable Energy Laboratory, Tech. Rep. NREL/CP-5500-49303, October 2010.

[12] J. E. Pacheco and R. Gilbert, "Overview of recent results of the solar two test and evaluations program," Sandia National Laboratories, Tech. Rep. SAND99-0091C, January 1999.

[13] U. Herrmann and D. W. Kearney, "Survey of thermal energy storage for parabolic trough power plants," *Journal of Solar Energy Engineering*, vol. 124, pp. 145–152, May 2002.

[14] P. W. Parfomak, "Energy storage for power grids and electric transportation: A technology assessment," Congressional Research Service, Tech. Rep. R42455, March 2012.

[15] D. W. Kearney, B. Kelly, U. Herrmann, R. Cable, J. E. Pacheco, A. R. Mahoney, H. Price, D. M. Blake, P. Nava, and N. Potrovitza, "Engineering aspects of a molten salt heat transfer fluid in a trough solar field," *Energy*, vol. 29, pp. 861–870, April-May 2004.

[16] A. Gil, M. Medrano, I. Martorell, A. Lázaro, P. Dolado, B. Zalba, and L. F. Cabeza, "State of the art on high temperature thermal energy storage for power generation. part 1—concepts, materials and modellization," *Renewable and Sustainable Energy Reviews*, vol. 14, pp. 31–55, January 2010.

[17] J. E. Pacheco, S. K. Showalter, and W. J. Kolb, "Development of a molten-salt thermocline thermal storage system for parabolic trough plants," *Journal of Solar Energy Engineering*, vol. 124, pp. 153–159, May 2002.

[18] D. L. Barth, J. E. Pacheco, W. J. Kolb, and E. E. Rush, "Development of a high-temperature, long-shafted, molten-salt pump for power tower applications," *Journal of Solar Energy Engineering*, vol. 124, pp. 170–175, May 2002.

[19] M. Medrano, A. Gil, I. Martorell, X. Potau, and L. F. Cabeza, "State of the art on high-temperature thermal energy storage for power generation. part 2—case studies," *Renewable and Sustainable Energy Reviews*, vol. 14, pp. 56–72, January 2010.

[20] P. Gilman, N. Blair, M. Mehos, C. B. Christensen, and S. Janzou, "Solar advisor model user guide for version 2.0," National Renewable Energy Laboratory, Tech. Rep. NREL/TP-670-43704, August 2008.

[21] R. Sioshansi and P. Denholm, "The value of concentrating solar power and thermal energy storage," *IEEE Transactions on Sustainable Energy*, vol. 1, pp. 173–183, October 2010.

[22] H. Price, "Parabolic trough solar power plant simulation model," National Renewable Energy Laboratory, Tech. Rep. NREL/CP-550-33209, January 2003.

[23] R. Sioshansi and P. Denholm, "The value of concentrating solar power and thermal energy storage," National Renewable Energy Laboratory, Tech. Rep. NREL/TP-6A2-45833, February 2010.

[24] R. Billinton and R. N. Allan, *Reliability Evaluation of Power Systems*. Boston: Pitman Advanced Publishing Program, 1984.

[25] M. R. Milligan and B. Parsons, "Comparison and case study of capacity credit algorithms for intermittent generators," National Renewable Energy Laboratory, Tech. Rep. NREL/CP-440-22591, March 1997.

[26] C. D'Annunzio and S. Santoso, "Noniterative method to approximate the effective load carrying capability of a wind plant," *IEEE Transactions on Energy Conversion*, vol. 23, pp. 544–550, June 2008.

[27] M. R. Milligan and K. Porter, "Determining the capacity value of wind: An updated survey of methods and implementation," National Renewable Energy Laboratory, Tech. Rep. NREL/CP-500-43433, June 2008.

[28] L. Söder and M. Amelin, "A review of different methodologies used for calculation of wind power capacity credit," in *2008 IEEE Power and Energy Society General Meeting*. Pittsburgh, PA, USA: Institute of Electrical and Electronics Engineers, 20-24 July 2008.

[29] C. Ensslin, M. R. Milligan, H. Holttinen, M. O'Malley, and A. Keane, "Current methods to calculate capacity credit of wind power, iea collaboration," in *2008 IEEE Power and Energy Society General Meeting*. Pittsburgh, PA, USA: Institute of Electrical and Electronics Engineers, 20-24 July 2008.

[30] M. Amelin, "Comparison of capacity credit calculation methods for conventional power plants and wind power," *IEEE Transactions on Power Systems*, vol. 24, pp. 685–691, May 2009.

[31] L. L. Garver, "Effective load carrying capability of generating units," *IEEE Transactions on Power Apparatus and Systems*, vol. PAS-85, pp. 910–919, August 1966.

[32] J. Haslett and M. Diesendorf, "The capacity credit of wind power: A theoretical analysis," *Solar Energy*, vol. 26, pp. 391–401, 1981.

[33] L. Söder and J. Bubenko, "Capacity credit and energy value of wind power in hydro-thermal power system," in *Proceedings of the 9th Power Systems Computation Conference*, Cascais, Portugal, 30 August-4 September 1987.

[34] A. Tuohy and M. O'Malley, "Impact of pumped storage on power systems with increasing wind penetration," in *Power & Energy Society General Meeting*. Calgary, Alberta, Canada: Institute of Electrical and Electronics Engineers, 26-30 July 2009, pp. 1–8.

[35] B. Hasche, A. Keane, and M. O'Malley, "Capacity value of wind power, calculation, and data requirements: the irish power system case," *IEEE Transactions on Power Systems*, vol. 26, pp. 420–430, February 2011.

[36] S. Bernow, B. Biewald, J. Hall, and D. Singh, "Modelling renewable electric resources: A case study of wind," Oak Ridge National Laboratory, Tech. Rep. ORNL/Sub-93-03370, July 1994.

[37] M. A. H. El-Sayed, "Substitution potential of wind energy in egypt," *Energy Policy*, vol. 30, pp. 681–687, June 2002.

[38] S. Pelland and I. Abboud, "Comparing photovoltaic capacity value metrics: A case study for the city of Toronto," *Progress in Photovoltaics: Research and Applications*, vol. 16, pp. 715–724, December 2008.

[39] R. Sioshansi, P. Denholm, T. Jenkin, and J. Weiss, "Estimating the value of electricity storage in PJM: Arbitrage and some welfare effects," *Energy Economics*, vol. 31, pp. 269–277, March 2009.
[40] E. P. Kahn, "Effective load carrying capability of wind generation: Initial results with public data," *The Electricity Journal*, vol. 17, pp. 85–95, December 2004.
[41] "20% wind energy by 2030: Increasing wind energy's contribution to U.S. electricity supply," U.S. Department of Energy, Tech. Rep. DOE/GO-102008-2567, July 2008.
[42] P. Denholm and R. Sioshansi, "The value of compressed air energy storage with wind in transmission-constrained electric power systems," *Energy Policy*, vol. 37, pp. 3149–3158, August 2009.
[43] S. Wilcox, "National solar radiation database 1991-2005 update: User's manual," National Renewable Energy Laboratory, Tech. Rep. NREL/TP-581-41364, April 2007.
[44] D. Finon and V. Pignon, "Capacity mechanisms in imperfect electricity markets," *Utilities Policy*, vol. 16, pp. 141–142, September 2008.
[45] *Methods to Model and Calculate Capacity Contributions of Variable Generation for Resource Adequacy Planning*, North American Electric Reliability Corporation, Princeton, New Jersey, March 2011.

Seyed Hossein Madaeni (S'11) is a Ph.D. candidate in the Integrated Systems Engineering Department at The Ohio State University. His research focuses on renewable energy analysis and restructured power systems. He holds a B.S. and an M.S. in electrical engineering from the University of Tehran.

Ramteen Sioshansi (M'11) is an assistant professor in the Integrated Systems Engineering Department at The Ohio State University. His research focuses on renewable and sustainable energy system analysis and the design of restructured competitive electricity markets.

He holds a B.A. in economics and applied mathematics and an M.S. and Ph.D. in industrial engineering and operations research from the University of California, Berkeley, and an M.Sc. in econometrics and mathematical economics from The London School of Economics and Political Science.

Paul Denholm (M'11–SM'12) is a senior analyst in the Strategic Energy Analysis Center at the National Renewable Energy Laboratory. His research interests are in the effects of large-scale renewable energy deployment in electric power systems, and renewable energy enabling technologies such as energy storage and long distance transmission.

He holds a B.S. in physics from James Madison University, an M.S. in instrumentation physics from the University of Utah, and a Ph.D. in land resources/energy analysis and policy from the University of Wisconsin-Madison.